ATL-TILECAL-2001-005
02/10/2001

COMPARATIVE ANALYSIS OF THE ATLAS TILE HADRONIC CALORIMETER RESPONSE TO PIONS AND PROTONS

S.Constantinescu[b], **S.Dita**[b], **A.Henriques**[c], **M.Nessi**[c], **R.Stanek**[a]

[a] *Argonne National Laboratory, USA*
[b] *Institute of Atomic Physics, Bucharest, Romania*
[c] *CERN, Geneva, Switzerland*

Abstract: A comparative analysis of the calorimeter response to pions and protons has been done using positive pion beams obtained in the H8 beam line at SPS where among pions there is also a significant amount of protons and muons. The separation between protons, pions and muons have been done using the Cerenkov Counter and the energy deposited in calorimeter. The differences which have been observed in the pion and proton response : a higher response and a better linearity for pions as well as a better resolution for protons, can be well understood by the existence of a pure hadronic fraction for pions smaller than the pure hadronic fraction for protons. The obtained experimental results are in good agreement with the Monte Carlo simulations.

Contents

1. INTRODUCTION

The crucial role played by hadron calorimeters in the new generation of high energy experiments is unanimously recognised. The better understanding of the physics on which these hadron calorimeters are based and the analysis of the factors that determine their performances present a special interest and can be very useful in improving the existing simulation codes for hadronic showers.
In this note the first results of our comparative analysis of the Tile Calorimeter response to pions and protons are presented together with a detailed comparison of the experimental data with the predictions based on the G-CALOR hadronic shower simulation package [2].
During the first beam tests dedicated to the two extended pre-series modules of Tile Calorimeter (modules zero), the pressure of the Cerenkov Counter , present in the H8 beam line, was set to a value lower than the proton threshold corresponding to the current incident energy. The goal was to estimate the amount of protons present in the positive pion beams at this beam line.
Taking into account the Cerenkov signal and the energy deposition in the calorimeter modules, the separation of pions, protons and muons in the beam energy interval $50 \leq E_{beam} \leq 180$ GeV has been performed and the significant amounts of protons observed in the positive pion beams have offered us the opportunity to develop a comparative analysis of the Tile Calorimeter response to pions and protons.
In 1998, the barrel module zero was tested with five one meter prototypes placed on either sides (in ϕ) of module 0 to ensure the hadronic shower containment.
The high amounts of protons in the H8 positive pion beams, obtained using the 1998 data, confirmed our previous results and gave us the possibility to continue, but this time more extensively, our comparative analysis of the different response to pions and protons.
Thus, in this note we present the results of our comparative analysis of Tile Calorimeter response to pions and protons based on the 1998 barrel module zero data. In section 2 we discuss how the separation of protons from pions was performed and the results we have obtained. In section 3 the estimated values of the ratio between pion and proton response are presented and compared with predictions based on simulations. In section 4 the relative non-linearity and the energy resolution obtained for pions and protons are presented and compared with simulations. An outlook is given in section 5.

2. SEPARATION OF PIONS AND PROTONS

To separate protons from pions, the H8 beam line Cerenkov Counter has been used. The pressure of the Cerenkov Counter [1] has to be set to a value :
a) lower than the proton threshold for the current incident energy

and
b) assuring a high efficiency of the Cerenkov Counter to pions.
For an efficient separation between protons and pions both conditions have to be fulfilled and as a consequence the separation was possible only in the beam energy interval $50 \leq E_{beam} \leq 180$ GeV.
In Figure 1, we present the distributions of the Cerenkov signal obtained at a pseudorapidity value equal to $\eta = -0.45$, for a pressure value of the Cerenkov Counter slightly lower than the proton threshold, at the four beam energies which present interest for our analysis.
We can clearly separate two groups of particles :
a) the group of particles with Cerenkov signal near zero which we identified as protons (and some background) and
b) the group of particles with a higher Cerenkov signal - pions, muons and electrons.
At the other η values, taken into account in the present analysis, similar distributions with the ones shown in Figure 1 have been obtained.
At 180 GeV, the pion efficiency is no longer one, at a pressure value lower than the proton threshold, and thus the separation between pions and protons at this incident energy has some ambiguity; in the protons samples one finds pions (about 5% from all the pions) due to the Cerenkov Counter inefficiency.
Kaons, which are also present in the positive pion beams, will go together with pions or protons as a function of their incident energy and the pressure value of the Cerenkov Counter. At 50 GeV, the pressure of the Cerenkov Counter was set to a value lower than the kaon and proton threshold. There the efficiency for pions is nearly one and thus we know that among protons we count also kaons. For the other energies used in our analysis, the pressure of the Cerenkov Counter was set at values higher than the kaon threshold and the kaons are mixed with pions.
In order to make a more accurate separation, e.g. to identify protons, kaons, pions and electrons present in the positive pion beams obtained in the H8 beam line, in a future test beam setup the installation of a second Cerenkov Counter is foreseen.
In Figure 2, we present the bidimensional distributions representing the correlation between the deposited energy and the Cerenkov signal at η = - 0.45 for the investigated beam energies. Three groups of events can be clearly seen (neglecting the background) :
a) the muons - with small energy deposition in the calorimeter and high Cerenkov signal,
b) the pions - with high energy deposition in the calorimeter and high Cerenkov signal and
c) the protons - with high energy deposition and small Cerenkov signal.
Again, distributions similar to the ones presented in Figure 2 have been obtained for the other pseudorapidity values.
In Figure 3 we present the result of our separation, i.e. the fraction of muons, pions and protons in the positive pion beams as a function of the beam energy.
As it can be seen, the plotted fractions present strong variations as the incident energy increases. If at 50 GeV incident energy, the fraction of pions is twice as much as the fraction of protons, at 100 GeV the two fractions are nearly equal, while at 180 GeV the fraction of protons is two times higher. The fraction of muons is smaller than the proton

and pion ones, less than 16% at all the incident energies with the exception of 100 GeV where a value of about 30% has been reached, a value close to the fraction of pions. It is worth mentioning that the fractions obtained previously, using the data from extended barrel beam tests, are in good agreement with the fractions presented in Figure 3. Thus, our more recent results confirm the presence in the positive pion beams at H8 beam line of a significant amount of protons.
The H8 beam is a secondary particle beam that provides hadrons, electrons or muons of energy between 10 and 400 GeV as well as 450 GeV protons. The positive pion beam at the highest incident energy used in our analysis, e.g. 180 GeV, is a secondary beam while at 50, 80 and 100 GeV incident energy the positive pion beams are tertiary. For tertiary beam of pions, a target of Polyethylene was used as well as a lead absorber to remove the electron contamination.

3. THE RATIO BETWEEN PION AND PROTON RESPONSE

The deposited energy distributions for separated pions and protons are presented in Figure 4 for 50 GeV and 180 GeV (the highest and lowest beam energy used in our analysis) at a pseudorapidity value equal to η = - 0.45. For pions a higher value of the mean deposited energy can be observed with respect to protons.
In table 1, 2, and 3, the peak and the σ values from Gaussian fits over a $\pm 2\sigma$ range to raw pion and proton deposited energy spectra [4] are shown for all the beam energies used in our analysis and pseudorapidites : - 0.25, - 0.45, and - 0.65. Also presented in Table 1, 2, and 3 are the ratios σ/E.
It can be seen that for all the beam energies and for all the pseudorapidities, the mean value of the energy deposition is higher for pions than for protons and we will analyse in more details this effect when the π/p ratio - the ratio between the pion and proton response - will be discussed .
The σ value and the ratio σ/E are also higher for pions than for protons. The σ values for pions are higher than the corresponding values for protons with a percentage varying from 8 to 23, while the differences between the ratios σ/E for pions and protons are a little smaller due to the higher energy deposition of pions in our calorimeter.
In Figure 5 the energy dependence of the ratio π/p is presented. A higher signal for pions than for protons, as can be seen from Tables 1-3, determines a ratio π/p greater than one for all studied incident energies and pseudorapidities. All the values obtained for the ratios π/p are inside the interval $1.02 < \pi/p < 1.05$, showing that the values of the ratio π/p are higher than unity with few percents. The slow decrease of the ratio π/p with increasing energy can be observed for all the pseudorapidity values taken into account.
The values obtained from G-CALOR simulations are also shown in Figure 5 and a good agreement between the data and G-CALOR predictions can be seen.

In Figure 6, the pseudorapidity dependence of the ratio π/p is represented for the four incident energies used in the present analysis and no dependence on pseudorapidity can be seen. There is a good agreement between the data and G-CALOR simulations concerning the pseudorapidity dependence of the π/p ratio with one exception - the 80 GeV point for η = - 0.35.
Simulations with different hadronic shower codes[6],[7],[8], [9], have suggested a power law description of the pure hadronic energy fraction :

$$F_h(E) = (E/E_0)^{m-1} \tag{3.1}$$

where E_0 is the extrapolated energy at which the hadronic fraction would reach unity.
For different targets and incident particles small variations of the parameter m have been obtained by fits to the hadronic energy fraction of the Eq. (3.1) and it was concluded that power laws with values for the parameter m about 0.85 provided a good description of all high-energy data [5].
Gabriel and al.[5], using CALOR simulations, have determined the following values of the parameters m and E_0 for incident pions and protons on iron target :

$$m = 0.816 \;\; E_0 = 0.96 \quad \text{for pions} \tag{3.2}$$

$$m = 0.814 \;\; E_0 = 2.62 \quad \text{for protons} \tag{3.3}$$

Using the relation :

$$F_{\pi^0}^{\pi(p)}(E) = 1 - F_h^{\pi(p)}(E) \tag{3.4}$$

and the parameterisations (3.2)-(3.3) we have obtained the energy dependence of the electromagnetic energy fraction for pions and protons - $F_{\pi^0}^{\pi}(E)$ and $F_{\pi^0}^{p}(E)$. Comparing the Wigmans parameterisation for the electromagnetic fraction :

$$F_{\pi^0}^{W}(E) = 0.11\, ln\, E \tag{3.5}$$

to $F_{\pi^0}^{\pi}(E)$ and $F_{\pi^0}^{p}(E)$, we have observed that $F_{\pi^0}^{W}(E)$ fulfils the relation :

$$F_{\pi^0}^{p}(E) \leq F_{\pi^0}^{W}(E) \leq F_{\pi^0}^{\pi} \tag{3.6}$$

in the energy interval $20 < E < 500$ GeV where the parameterisations (3.2) - (3.3) have given a good description of CALOR simulations.
According to (3.2) - (3.3), the values of the parameter m for pions and protons are practically equal and thus the ratio between the hadronic fraction of pions and protons of the same energy is a constant equal to :

$$\frac{F_h^{\pi}(E)}{F_h^{p}(E)} = 0.83 \tag{3.7}$$

The lower pure hadronic fraction of pions, which means according to (3.4) a higher electromagnetic fraction for pions, determines in the case of an non-compensating calorimeter with $e/h > 1$ a higher signal for pions than for protons of the same energy.

As the Tile Calorimeter is a non-compensating calorimeter with $e/h > 1$, a higher signal for pions is expected and indeed our data show clearly this effect as can be seen from Figures (4 and 5) and Tables 1-3.
Thus, our experimental data confirm the result obtained from Monte Carlo simulations by Gabriel and al.[5] concerning a larger electromagnetic fraction in a shower initiated by pions than by protons of the same energy.
The higher electromagnetic fraction of pions can be explained by the presence of the leading pion charge exchange mechanism in the case of incident charged pions.
By this mechanism, an important fraction of energy is removed from the hadronic sector of the pion shower.
Taking into account the non-compensation of our calorimeter and the parameterisations (3.2) - (3.3), we can calculate the π/p ratio and compare the obtained values to the experimental values.
To calculate the ratio π/p we have used the relation :

$$\pi/p = \frac{e/h + (1 - e/h)F_h^{\pi}(E)}{e/h + (1 - e/h)F_h^{p}(E)} \tag{3.8}$$

where

$$e/h = 1.36 \pm 0.11 \tag{3.9}$$

has been determined experimentally by studying the response of pions incident at $\theta = 20^0$ on our calorimeter [10].
Taking into account the e/h value given by Eq. (3.9) and using the relation (3.8) we have obtained the following values :

$$\pi/p = 1.030 \pm 0.008, \quad 1.027 \pm 0.007, \quad 1.025 \pm 0.006 \quad 1.022 \pm 0.005 \tag{3.10}$$

at 50, 80, 100 and 180 GeV, respectively.
Our experimental values for the π/p ratio at η = - 0.35 have been compared to the calculated values (3.10). A good agreement between the data and the calculations can be observed (see Figure 5).
The decrease of the π/p ratio with increasing energy can also be seen. This behaviour is expected according to the relation (3.8), the parameterisations (3.2) - (3.3) and the fact that our calorimeter is non-compensating with $e/h > 1$. Thus, there are several arguments in the favour of a good description of $F_h^{\pi}(E)$ and $F_h^{p}(E)$ by the parameterisations (3.2)-(3.3).
The higher σ values obtained experimentally for pions than for protons, as can be seen from Tables 1-3, can also be explained by the presence of the leading pion charge exchange mechanism in the pion shower. Due to this mechanism large non-Gaussian fluctuations are expected in the electromagnetic fraction (or F_h^{π}) of pions. These fluctuations are playing an important role in the calorimeter resolution as they determine - together with the degree of non-compensation of the calorimeter - the value of the constant term of the energy resolution, a term which is always present in the resolution of non-compensating calorimeters.

It is worth mentioning that the good agreement between the experimental values and the G-CALOR Monte Carlo predictions of the ratio π/p is also a confirmation of our efficient separation between pions and protons.

4. THE RELATIVE NON-LINEARITY AND THE ENERGY RESOLUTION

In our systematic comparison of the pion and proton response, an important role is played by the relative non-linearity and the energy resolution obtained at different pseudorapidity values.

In Figure 7, the normalised (to the 100 GeV point) relative non-linearity of the pion and proton response is shown as a function of the beam energy at different pseudorapidities (η = - 0.25, - 0.35, - 0.45, - 0.55, - 0.65). The very good linearity of the pion response can be seen. The non-linearity for pions is less than $\pm$ 1%.

G-CALOR predicts also a good linearity for pions ($\pm$ 2%) but the non-linearity is slightly higher than the one obtained experimentally.

For protons the non-linearity of the response is a little higher than for pions and the better linearity of pions as well in the data as in G-CALOR simulations can be observed in Figure 7. This result can be seen for all the energies and all the pseudorapidities taken into account in our analysis.

It presents also interest to calculate the non-linearity of the response using the parameterisations (3.2) and (3.3) and to compare the calculated values to the data. The relative non-linearity of pions of energy E (normalised to the response to pions of energy E_0) - $R_\pi(E)$ - is given by the relation:

$$R_\pi(E) = \frac{< E_\pi > /E_{nom}}{(< E_\pi > /E_{nom})_{E_0}} \tag{4.1}$$

and $R_\pi(E)$ can be calculated using the pure hadronic fraction of pions (F_h^π) by the relation :

$$R_\pi(E) = \frac{e/h + (1 - e/h)\, F_h^\pi(E)}{e/h + (1 - e/h)\, F_h^\pi(E_0)} \tag{4.2}$$

The energy variation of R_π can be written as :

$$dR_\pi/dE = c_\pi\,(1 - e/h)\, dF_h^\pi(E)/dE \tag{4.3}$$

where c_π is a constant :

$$c_\pi = \frac{1}{e/h + (1 - e/h)\, F_h^\pi(E_0)} \tag{4.4}$$

Now, in the relation (4.3) we can introduce the ratio between the pure hadronic fraction of pions and protons given by (3.7) and we obtain :

$$dR_\pi/dE = 0.83\, c_\pi\, (1 - e/h)\, dF_h^p(E)/dE \tag{4.5}$$

while the energy variation of the proton response (R_p) is given by :

$$dR_p/dE = c_p\, (1 - e/h)\, dF_h^p(E)/dE \tag{4.6}$$

where the constant c_p can be calculated using (4.4) after replacing $F_h^\pi(E_0)$ by $F_h^p(E_0)$.
One can see immediately that :

$$\frac{dR_\pi}{dE} < \frac{dR_p}{dE} \tag{4.7}$$

as $c_\pi < c_p$ due to the relation (3.7) and the fact that our calorimeter is non-compensating with $e/h > 1$ [10].
Thus, a smaller non-linearity for pions than for protons is expected using a non-compensating calorimeter with $e/h > 1$ due to the relation (3.7).
Using relation (4.2) and the parameterisation (3.2) we have calculated the non-linearity of the pion response for η = - 0.35 (the pseudorapidity for which the value of $e/h = 1.36 \pm 0.11$ has been determined experimentally) and in a similar way also the non-linearity of the proton response. The comparison between our data and the calculations are presented in Figure 8. A good agreement between the data and calculations can be observed.
The better linearity of the pion response seen as well in the data as in calculations represents another argument in the favour of the parameterisations (3.2) and (3.3). Thus, firstly we have observed a higher calorimeter response to pions than to protons of the same energy and we have considered that this is an experimental confirmation of the result of Gabriel et al. [5] concerning a smaller pure hadronic fraction for pions than for protons. Now, the experimental data concerning the linearity of the response to pions and protons, confirm once more the smaller pure hadronic fraction for pions than for protons and even more, the obtained data about the linearity can be used as an argument in the favour of a similar energy dependence for the two hadronic fractions $F_h^\pi(E)$ and $F_h^p(E)$, e.g. for a constant ratio - $F_h^\pi(E)/F_h^p(E) < 1$.
Within the goal to determine the intrinsic constant value e/h, we have fitted our data concerning the non-linearity of the response to pions with the relation (4.2). The obtained results were inconclusive as we have only four different incident energies.
Summing the total energy deposition in the calorimeter, without any correction for non-compensation, the energy dependence of the energy resolution shown in Figure 9 (Figure 10) at the pseudorapidity values equal to : η = - 0.25, - 0.45, (- 0.55, - 0.65) has been obtained.
The energy dependence of the energy resolution has been parameterised by the following formula :

$$\sigma/E = \frac{A}{\sqrt{E}} + B \tag{4.8}$$

where the resolution σ/E is in percent, the statistical term A is in $\%GeV^{1/2}$ and the constant term B is in percent. There is no noise term in the formula (4.8) since in Tile Calorimeter the noise contribution is negligible, about 40 MeV/per cell[11]. Figure 11 presents the η dependence of the statistical and constant terms, obtained by fit, from pion and proton data. The G-CALOR predictions are also shown and one can see a good agreement between the data and simulations for the statistical term of pions. For protons, Monte Carlo simulations are giving higher values for the statistical term at low pseudorapidity values.
Concerning the constant term, G-CALOR predicts smaller values than the data as well for pions as for protons. The differences between data and simulations are higher at lower pseudorapidity values.
It is a well known fact that G-CALOR hadronic package gives a degree of non-compensation smaller than the data and this can be an explanation for the observed smaller constant term in simulations.
Table 4 shows the values of these statistical and constant terms obtained for pions and protons at all the pseudorapidities used in this analysis.
Finally, at all the pseudorapidity values taken into account, a better energy resolution for protons than for pions can be observed as well in the data as in the G-CALOR simulations. As an example, we present in Figure 12, the η dependence of the energy resolution for pions and protons of 100 GeV and the better resolution of protons can be clearly seen.
This result can be explained by the large non-Gaussian fluctuations which are present in the purely electromagnetic component of the pion shower due to the leading charge exchange mechanism.
We intend to continue our study and to obtain from the data and G-CALOR simulations more information concerning the ratio between the purely hadronic component of the pion and proton shower (F_h^π / F_h^p).

5. CONCLUSION

The results presented in this paper have shown a significant amount of protons in the positive pion beams obtained at H8 beam line of SPS. This result have been obtained using two independent sets of test beam data taken in 1997 and 1998. The proton and pion fraction determined using the two independent sets of data are in a very good agreement.
Values above one were obtained for the π/p ratio for all the beam energies and all pseudorapidities taken into account in this analysis as was expected for a non-compensating calorimeter with $e/h > 1$ in the presence of a smaller pure hadronic fraction for pions than for protons. Thus it is possible to make the statement that our data confirm the existence of a smaller pure hadronic fraction for pions. A slow decrease of the ratio π/p with the increasing of the beam energy was observed as well as no dependence on pseudorapidity.
The good agreement between the data and G-CALOR Monte Carlo predictions

concerning the ratio π/p is also an argument in the favour of our efficient separation between pions and protons.
A better linearity for pions and a better energy resolution for protons is also an important result of our comparative analysis concerning pion and proton response. These results, shown by the data, are confirmed by the G-CALOR simulations.
We have shown that the better linearity for pions can be explained by the parameterisations proposed by [2] for the pure hadronic fraction of pions and protons. The parameterisations of [2] involved a constant ratio between the pure hadronic fraction of pions and protons and our data are confirming this result.
The observed resolution of pions worser than the one of protons can be explained by the large fluctuations existing in the electromagnetic fraction of pions due to charge exchange mechanism.

References

[1] D. Bartlett et al,Nucl. Inst. and Meth. A 260 (1987) 55

[2] T.A. Gabriel and C. Zeitnitz,Nucl. Inst. and Meth. A 349 (1994) 106

[3] D.E. Groom, SDC Collaboration Note SDC-93-559(1993)

[4] F. Ariztizabal et al.,Nucl. Inst. and Meth. A 349 (1994) 384

[5] T.A. Gabriel et al.,Nucl. Inst. and Meth. A 338 (1994) 336

[6] N.V.Mokhov and J.D.Cossairt, Nucl. Instr. and Meth. A244(1986) 349;

[7] T.Handler,P.K.Job,I.E. Price and T.A. Gabriel, SDC-92-257 (1992);

[8] P.A. Aarnio, A. Fasso, H.J.Mohring, J.Ranft, and G.R. Stevenson, CERN/TIS-RP/168(1986);

[9] P.A. Aarnio, A. Fasso, J.Lindgren, J.Ranft, and G.R. Stevenson, CERN/TIS-RP/190 (1987)

[10] RD-34 Collaboration CERN/LHCC 95-44

[11] A. Henriques Proceedings of the Sixth InternationalConference on Calorimetry in High Energy Physics

E_{Beam}	**PSEUDORAPIDITY = - 0.25**					
	PIONS			**PROTONS**		
(GeV)	$< Q >$ **(pC)**	σ **(pC)**	$\sigma / < Q >$ **(%)**	$< Q >$ **(pC)**	σ **(pC)**	$\sigma / < Q >$ **(%)**
50	41.24±0.08	4.32±0.07	10.47±0.17	39.36±0.09	3.51±0.07	8.92±0.18
80	66.26±0.13	6.12±0.12	9.24±0.18	63.68±0.11	5.38±0.09	8.45±0.14
100	82.16±0.30	7.41±0.18	9.02±0.22	80.31±0.14	6.28±0.12	7.82±0.15
180	146.90±0.34	11.04±0.32	7.52±0.22	144.16±0.24	9.62±0.21	6.67±0.15

Table 1: Peak and σ values from fits to raw pion and proton energy spectra at different beam energies and a pseudorapidity value equal to η = - 0.25.

E_{Beam}	**PSEUDORAPIDITY = - 0.45**					
	PIONS			**PROTONS**		
(GeV)	$< Q >$ **(pC)**	σ **(pC)**	$\sigma / < Q >$ **(%)**	$< Q >$ **(pC)**	σ **(pC)**	$\sigma / < Q >$ **(%)**
50	41.94±0.07	4.06±0.06	9.68±0.14	40.00±0.09	3.66±0.07	9.15±0.18
80	66.74±0.13	6.14±0.11	9.20±0.17	64.43±0.11	5.34±0.09	8.29±0.14
100	83.58±0.19	7.04±0.17	8.42±0.20	80.84±0.14	6.06±0.11	7.50±0.14
180	150.09±0.34	11.05±0.33	7.36±0.22	147.18±0.23	9.41±0.20	6.39±0.14

Table 2: Peak and σ values from fits to raw pion and proton energy spectra at different beam energies and a pseudorapidity value equal to η = - 0.45.

E_{Beam}	**PSEUDORAPIDITY = - 0.65**					
	PIONS			**PROTONS**		
(GeV)	$< Q >$ **(pC)**	σ **(pC)**	$\sigma / < Q >$ **(%)**	$< Q >$ **(pC)**	σ **(pC)**	$\sigma / < Q >$ **(%)**
50	43.34±0.07	3.98±0.05	9.18±0.12	41.63±0.09	3.70±0.07	8.89±0.17
80	69.12±0.12	5.97±0.11	8.64±0.16	66.87±0.10	4.88±0.08	7.30±0.12
100	86.32±0.19	6.84±0.16	7.92±0.19	83.85±0.13	5.84±0.11	6.96±0.13
180	155.35±0.38	11.22±0.33	7.22±0.21	152.78±0.27	9.21±0.19	6.03±0.12

Table 3: Peak and σ values from fits to raw pion and proton energy spectra at different beam energies and a pseudorapidity value equal to η = - 0.25.

η	**PIONS**				**PROTONS**			
	DATA		G-CALOR		DATA		G-CALOR	
	A $\%GeV^{1/2}$	**B** %	**A** $\%GeV^{1/2}$)	**B** (%)	**A** ($\%GeV^{1/2}$)	**B** (%)	**A** ($\%GeV^{1/2}$)	**B** (%)
-0.25	36.57 ±2.18	5.26 ±0.25	37.97 ±7.04	3.17 ±0.77	44.91 ±3.98	3.4 ±0.43	55.39 ±5.10	0.79 ±0.50
-0.35	30.17 ±4.10	6.14 ±0.48	35.14 ±5.27	3.34 ±0.55	29.91 ±4.05	4.96 ±0.44	44.22 ±4.71	1.64 ±0.48
-0.45	30.13 ±3.00	5.48 ±0.31	34.69 ±6.28	4.11 ±0.68	40.18 ±2.58	3.41 ±0.28	38.31 ±4.77	2.64 ±0.49
-0.55	38.22 ±3.91	4.25 ±0.44	31.10 ±6.24	3.80 ±0.66	34.40 ±4.14	3.76 ±0.47	34.77 ±4.50	2.59 ±0.47
-0.65	31.48 ±3.40	4.79 ±0.38	33.30 ±5.71	3.66 ±0.61	40.78 ±3.42	2.83 ±0.38	33.46 ±3.42	2.51 ±0.38

Table 4: Terms of the pion and proton energy resolution for the barrel module zero of the Tile Calorimeter obtained by fitting the test beam data at different pseudorapidities with the formula σ/E=A/$\sqrt{}$(E)+B. Also shown are the terms predicted by G-CALOR Monte Carlo.

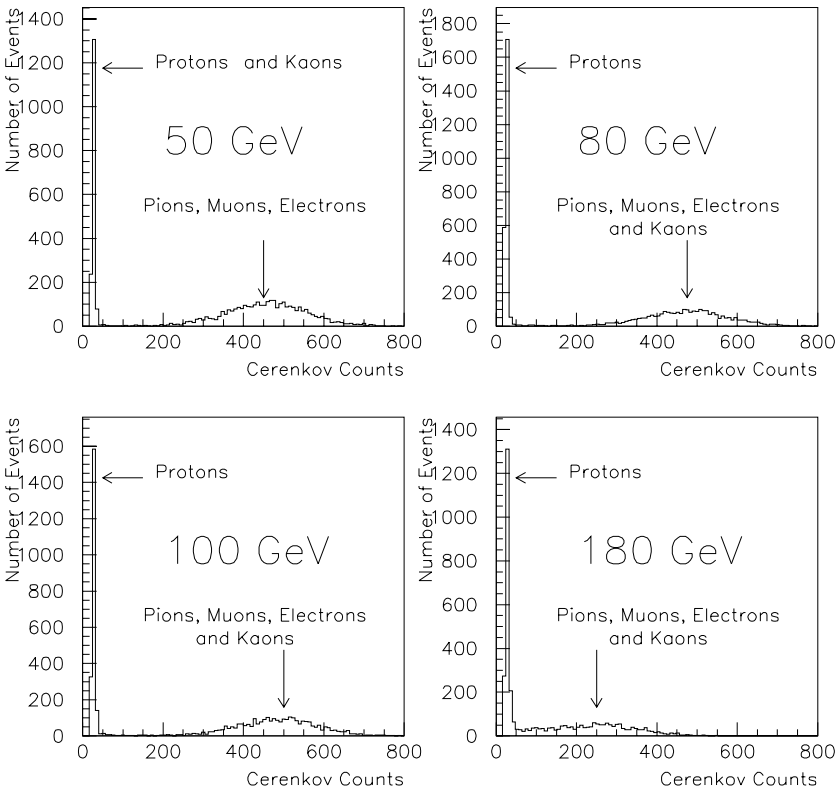

Figure 1: The Cerenkov signal distributions for the four beam energies where the separation between pions and protons has been done.

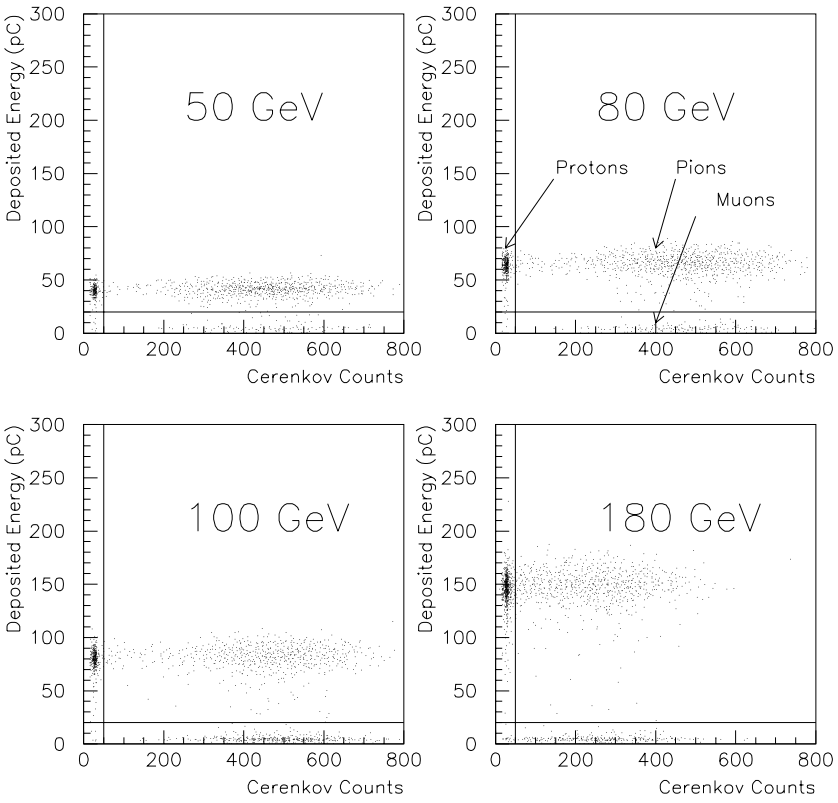

Figure 2: The correlation between the Cerenkov signal and the deposited energy for the four beam energies taken into account.

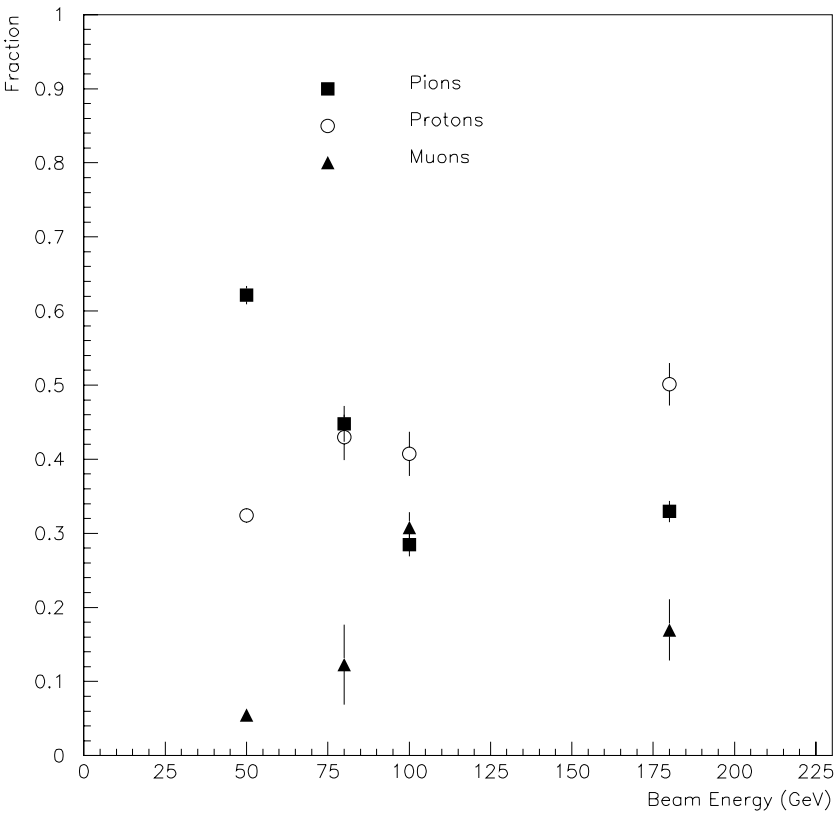

Figure 3: The fractions of pions, protons and muons in the positive pion beam function of beam energy.

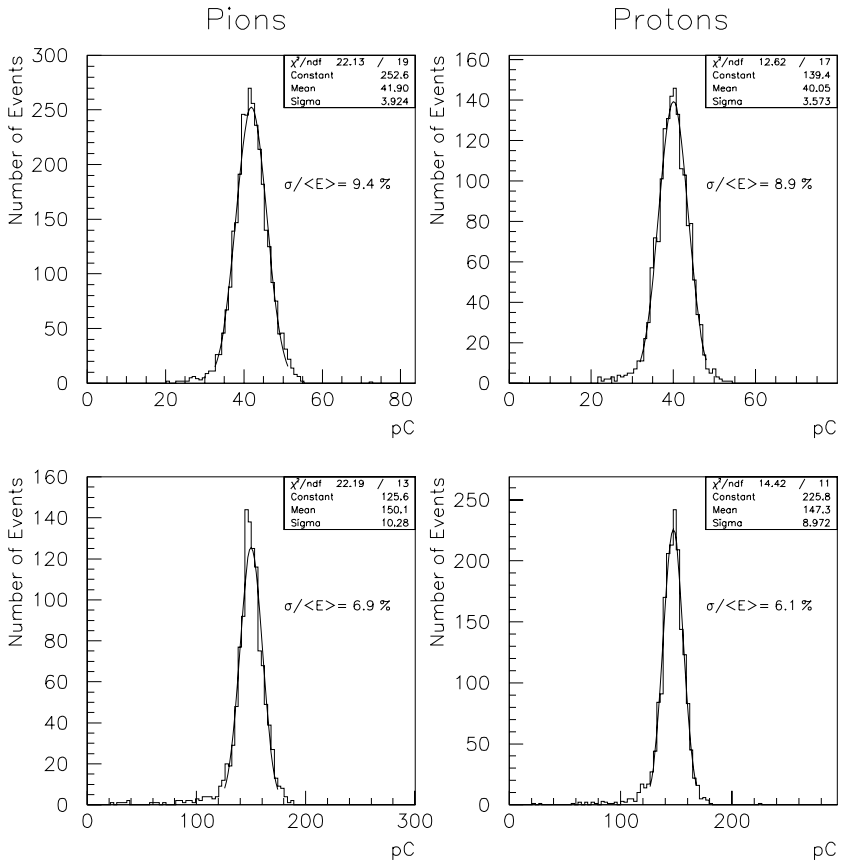

Figure 4: The deposited energy distributions for pions and protons at 50 and 180 GeV beam energy.

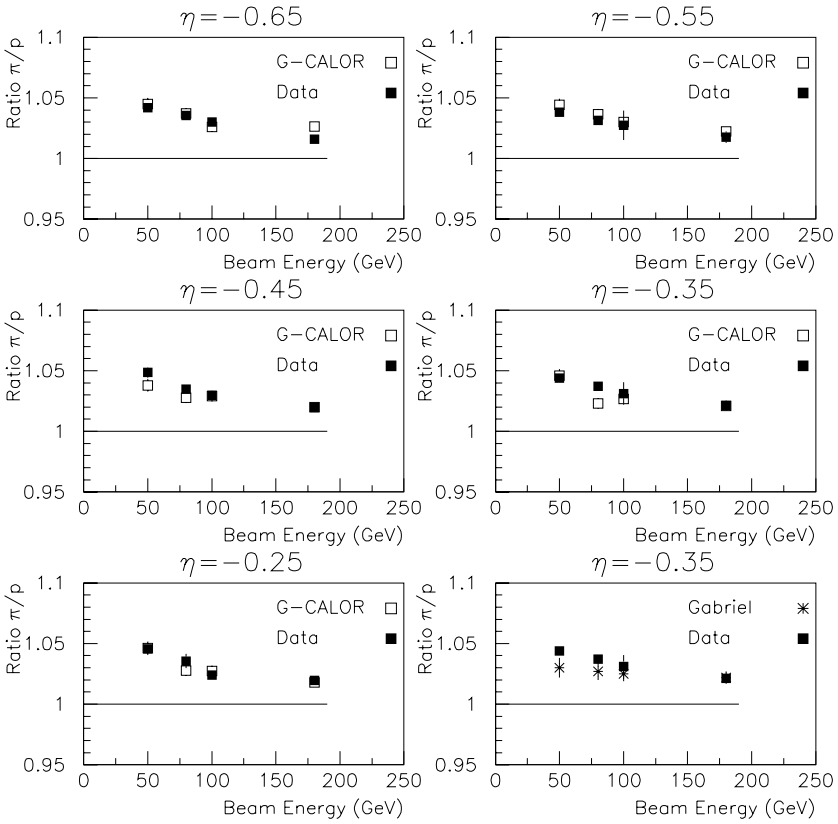

Figure 5: The beam energy dependence of the ratio π/p at different pseudorapidity values.

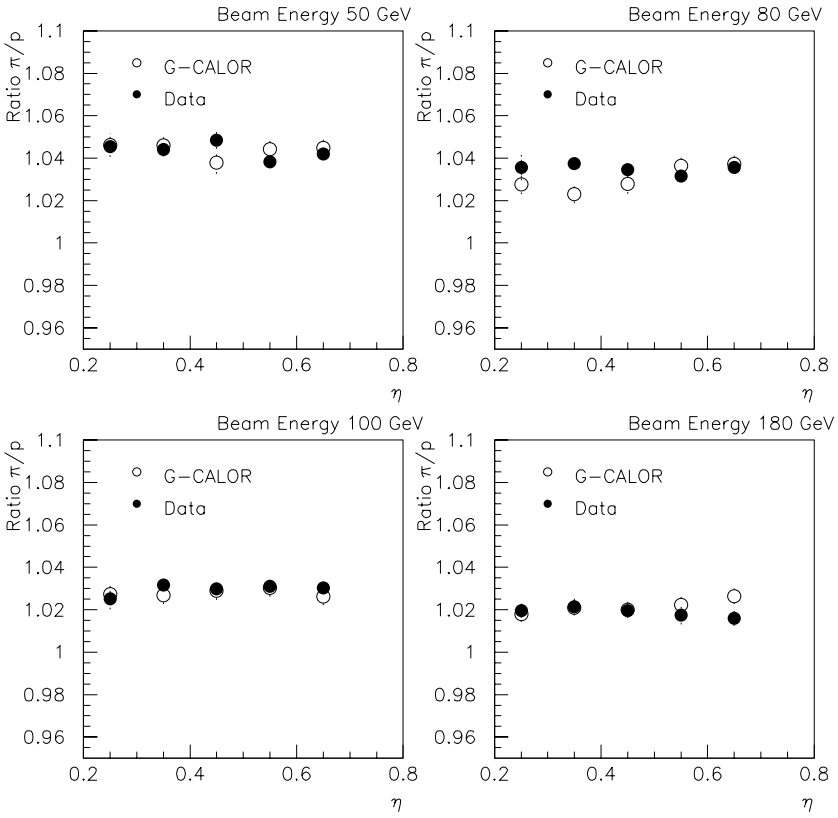

Figure 6: The η dependence of the ratio π/p for the four beam energies.

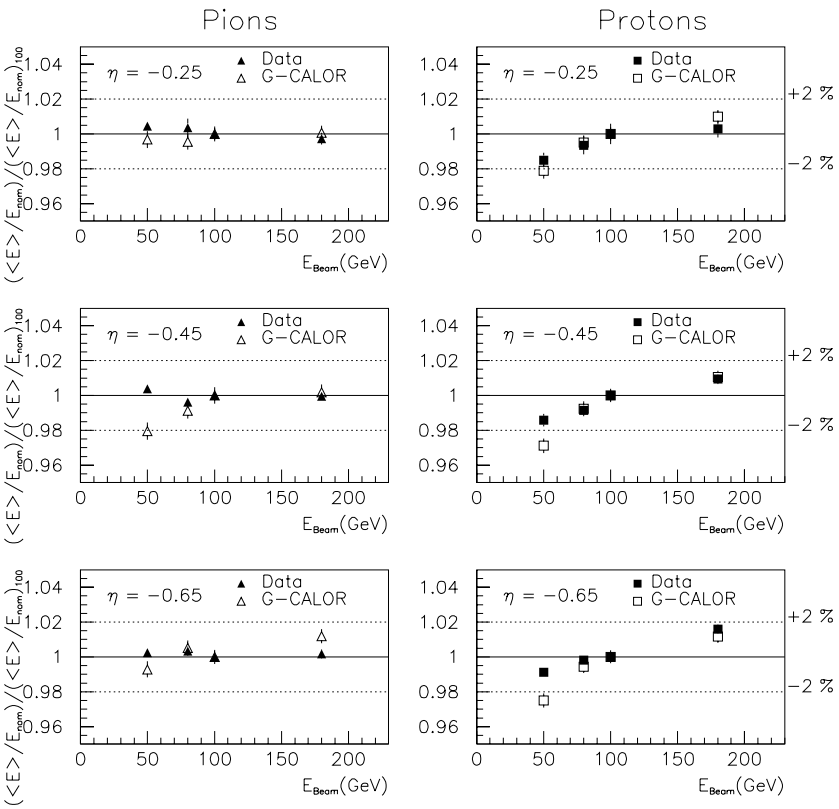

Figure 7: The normalised (to the 100 GeV point) relative non-linearity of pion and proton response as a function of beam energy at different pseudorapidities.

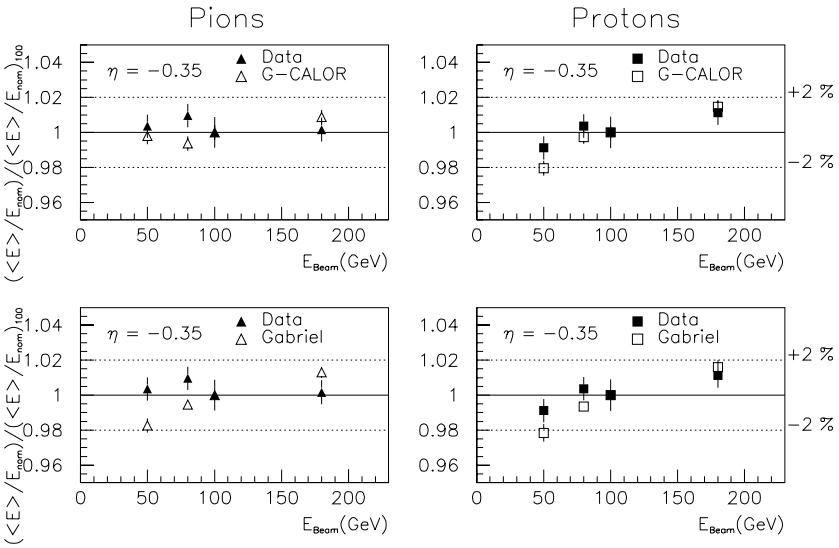

Figure 8: The normalised (to the 100 GeV point) relative non-linearity of pion and proton response as a function of beam energy at different pseudorapidities.

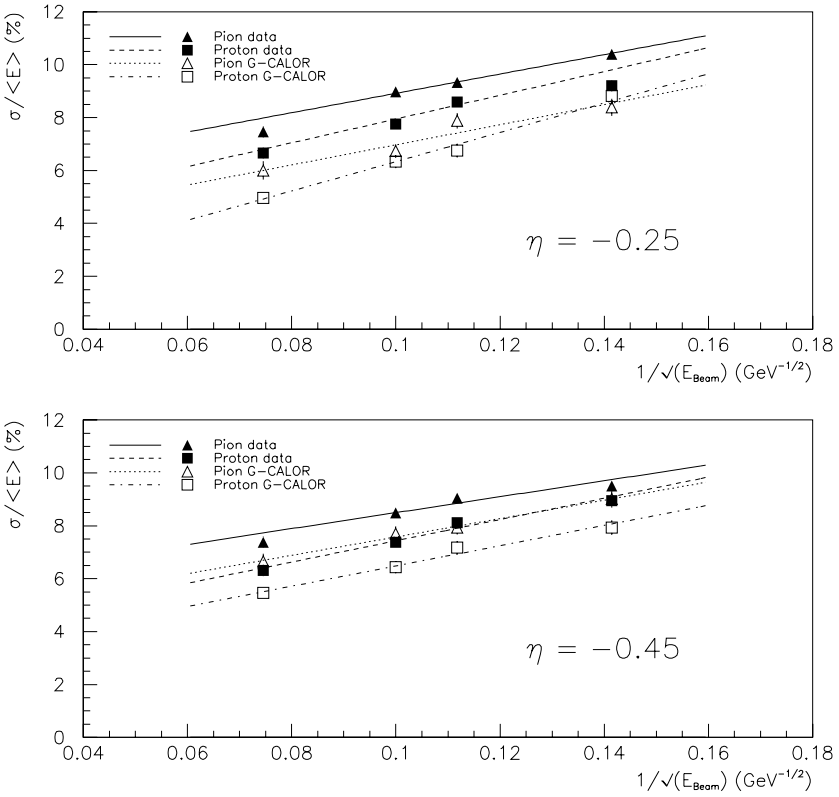

Figure 9: The energy dependence of the energy resolution for pions and protons at η = - 0.25 and η = - 0.45.

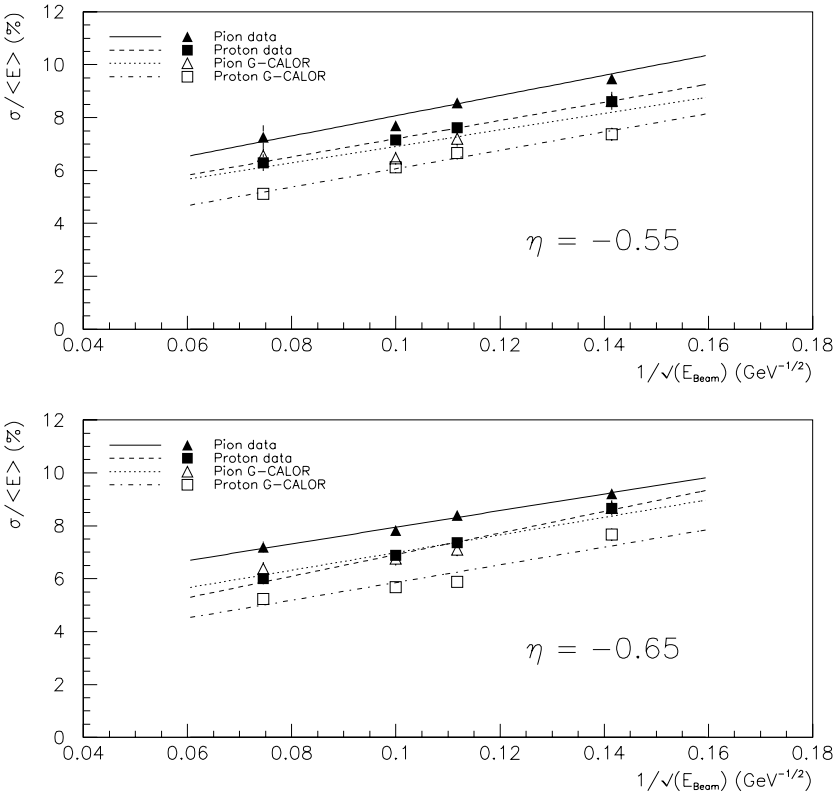

Figure 10: The energy dependence of the energy resolution for pions and protons at η = - 0.55 and η = - 0.65.

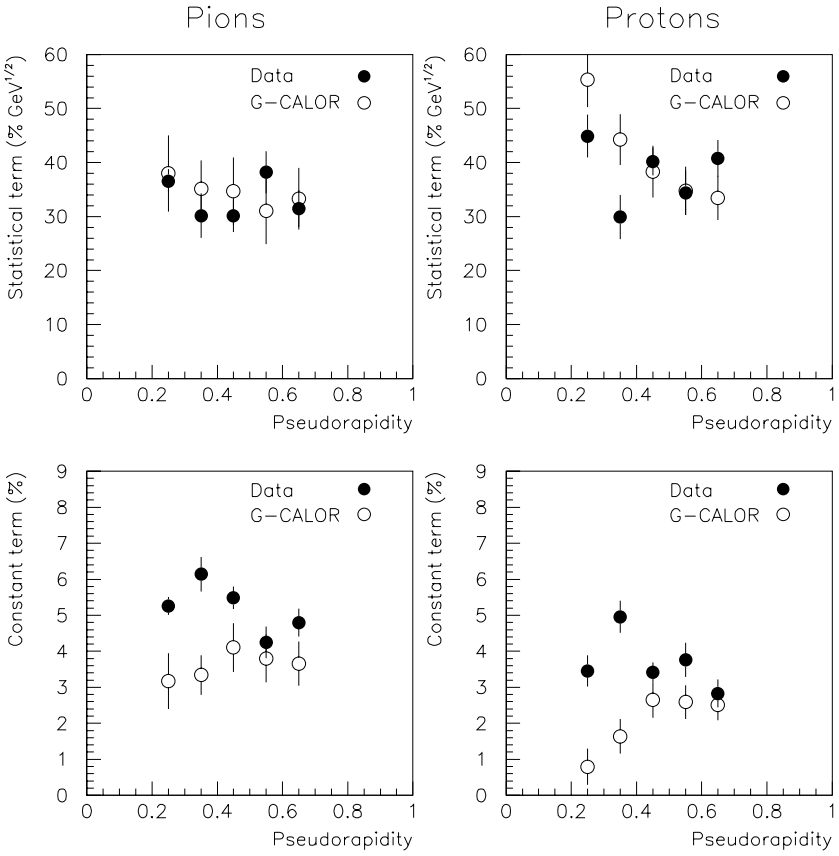

Figure 11: The η dependence of the statistical and constant terms of the energy resolution for pions and protons.

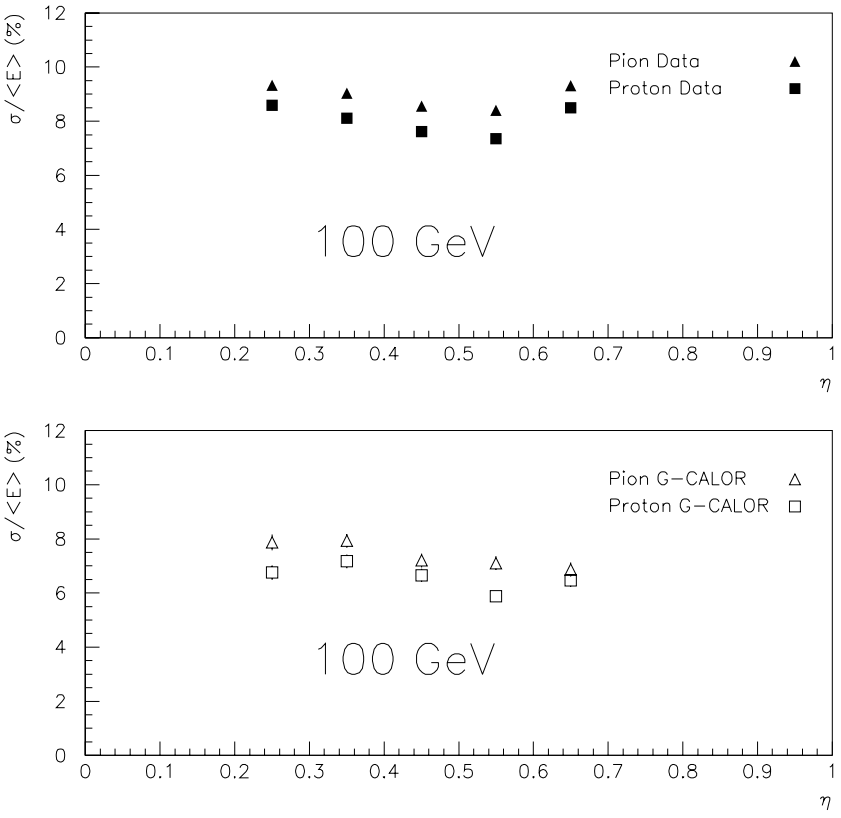

Figure 12: The η dependence of energy resolution for pions and protons at 100 GeV beam energy.